Hydrazonophenol, a Food Vacuole-Targeted and Ferriprotoporphyrin IX-Interacting Chemotype Prevents Drug-Resistant Malaria

CITATIONS
4

READS
304

10 authors, including:

Shubhra Jyoti Saha
Massachusetts Institute of Technology
12 PUBLICATIONS   **233** CITATIONS

SEE PROFILE

Asim Azhar Siddiqui
Nanyang Technological University
12 PUBLICATIONS   **277** CITATIONS

SEE PROFILE

Saikat Pramanik
Indian Institute of Chemical Biology
5 PUBLICATIONS   **66** CITATIONS

SEE PROFILE

Debanjan Saha
Indian Institute of Chemical Biology
5 PUBLICATIONS   **89** CITATIONS

SEE PROFILE

Some of the authors of this publication are also working on these related projects:

Characterization of ALBA family proteins in Plasmodium View project

All content following this page was uploaded by Asim Azhar Siddiqui on 28 January 2019.

The user has requested enhancement of the downloaded file.

Hydrazonophenol, a Food Vacuole-Targeted and Ferriprotoporphyrin IX-Interacting Chemotype Prevents Drug-Resistant Malaria

Shubhra Jyoti Saha, Asim Azhar Siddiqui, Saikat Pramanik, Debanjan Saha, Rudranil De, Somnath Mazumder, Subhashis Debsharma, Shiladitya Nag, Chinmoy Banerjee, and Uday Bandyopadhyay*

Division of Infectious Diseases and Immunology, CSIR - Indian Institute of Chemical Biology, 4 Raja S. C. Mullick Road, Jadavpur, Kolkata 700032, West Bengal, India

S Supporting Information

ABSTRACT: The rapid emergence of resistance against frontline antimalarial drugs essentially warrants the identification of new-generation antimalarials. Here, we describe the synthesis of (E)-2-isopropyl-5-methyl-4-((2-(pyridin-4-yl)hydrazono)methyl)phenol (**18**), which binds ferriprotoporphyrin-IX (Fe^{III}-PPIX) (K_d = 33 nM) and offers antimalarial activity against chloroquine-resistant and sensitive strains of *Plasmodium falciparum* in vitro. Structure–function analysis reveals that compound **18** binds Fe^{III}-PPIX through the −C=N−NH− moiety and 2-pyridyl substitution at the hydrazine counterpart plays a critical role in antimalarial efficacy. Live cell confocal imaging using a fluorophore-tagged compound confirms its accumulation inside the acidic food vacuole (FV) of *P. falciparum*. Furthermore, this compound concentration-dependently elevates the pH in FV, implicating a plausible interference with Fe^{III}-PPIX crystallization (hemozoin formation) by a dual function: increasing the pH and binding free Fe^{III}-PPIX. Different off-target bioassays reduce the possibility of the promiscuous nature of compound **18**. Compound **18** also exhibits potent in vivo antimalarial activity against chloroquine-resistant *P. yoelii* and *P. berghei* ANKA (causing cerebral malaria) in mice with negligible toxicity.

KEYWORDS: *Plasmodium*, malaria, hemozoin, food vacuole, parasite metabolism
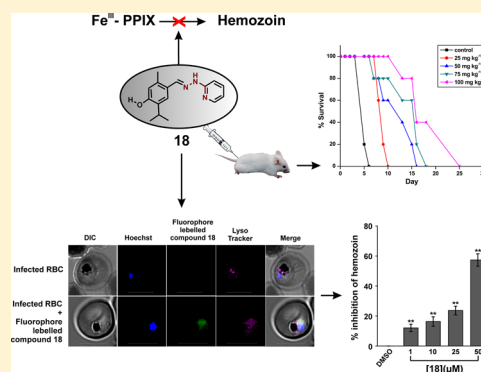
The adverse effect of malaria across the globe demands serious attention due to the increasing number of reports of multi-drug-resistant (MDR) strains posing a severe threat to human life and productivity.[1,2] Reports of 216 million cases with 445 000 deaths in 2016 repeatedly accentuate the desideratum of new antimalarial chemotherapeutics against MDR strains.[3] Moreover, the emergence of drug resistance against artemisinin partner drugs such as piperaquine and mefloquine has resulted in a significant failure of artemisinin combination therapy (ACT) on the Thai−Cambodian border, where chloroquine (CQ) resistance was developed almost 50 years ago.[4] The spread of resistance therefore needs to be dealt with in the identification of new antimalarial chemotypes that are efficacious against MDR malaria in the most unfortified regions.[1,5]

Intraerythrocytic stages of *P. falciparum* are responsible for its clinical symptoms, and during these stages, the parasite digests hemoglobin in the acidic food vacuole (FV) and thereby releases heme (Fe^{III}-PPIX), a nonprotein constituent of hemoglobin as a byproduct.[6,7] This free Fe^{III}-PPIX, a well-known pro-oxidant, may cause severe oxidative damage to the lipid bilayers of the parasitic cell membrane, leading to membrane lesion.[8−10] In order to evade the detrimental consequences of free Fe^{III}-PPIX accumulation, *Plasmodium* crystallizes it into nontoxic inert hemozoin (Hz).[11,12] It was found that the development of CQ resistance in parasites was mainly due to multiple mutations in the *P. falciparum* CQ resistance transporter (*Pf*CRT) that results in structure-specific efflux of the drug from FV.[13] Despite this resistance, the Hz crystallization pathway within the parasite is still essential, and thus it may be used as a sustainable drug target.[14] Thus, scaffolds which bind to free Fe^{III}-PPIX and inhibit Hz crystallization can be detrimental to parasites due to free Fe^{III}-PPIX accumulation within the FV and have merit as potent antimalarials.

In the search for new antimalarial chemotypes, we focused our study on Fe^{III}-PPIX binding moieties that are capable of interacting with high affinity. A novel class of chiral gallium(III) complexes of amine-phenol ligand and schiff-base phenol ligand were reported to possess decent efficacy against CQ-sensitive and -resistant strains.[15] These cationic
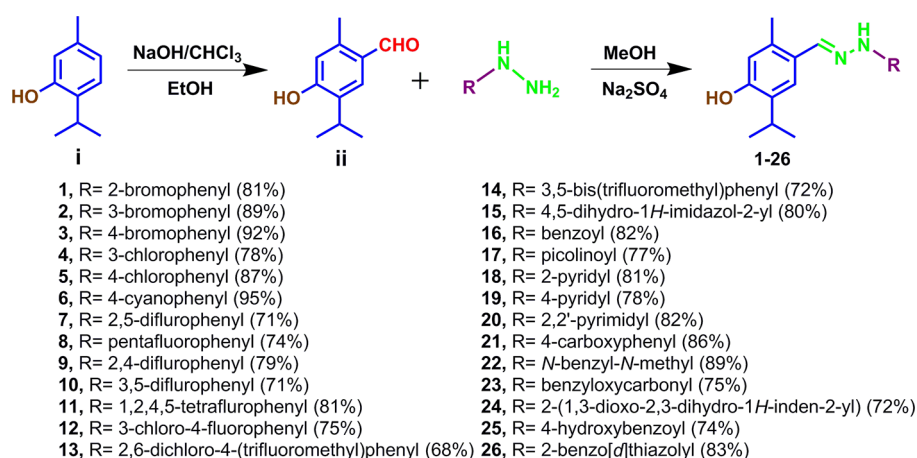
Figure 1. Synthesis of hydrazonophenols. Percentages in parentheses represent yields.

1, R= 2-bromophenyl (81%)
2, R= 3-bromophenyl (89%)
3, R= 4-bromophenyl (92%)
4, R= 3-chlorophenyl (78%)
5, R= 4-chlorophenyl (87%)
6, R= 4-cyanophenyl (95%)
7, R= 2,5-diflurophenyl (71%)
8, R= pentaflurophenyl (74%)
9, R= 2,4-diflurophenyl (79%)
10, R= 3,5-diflurophenyl (71%)
11, R= 1,2,4,5-tetraflurophenyl (81%)
12, R= 3-chloro-4-fluorophenyl (75%)
13, R= 2,6-dichloro-4-(trifluoromethyl)phenyl (68%)

14, R= 3,5-bis(trifluoromethyl)phenyl (72%)
15, R= 4,5-dihydro-1*H*-imidazol-2-yl (80%)
16, R= benzoyl (82%)
17, R= picolinoyl (77%)
18, R= 2-pyridyl (81%)
19, R= 4-pyridyl (78%)
20, R= 2,2'-pyrimidyl (82%)
21, R= 4-carboxyphenyl (86%)
22, R= *N*-benzyl-*N*-methyl (89%)
23, R= benzyloxycarbonyl (75%)
24, R= 2-(1,3-dioxo-2,3-dihydro-1*H*-inden-2-yl) (72%)
25, R= 4-hydroxybenzoyl (74%)
26, R= 2-benzo[*d*]thiazolyl (83%)

complexes have been proposed to inhibit hemozoin formation via the specific drug/Fe^{III}-PPIX interaction. Different Schiff base phenol, amine phenol, and Schiff base naphthalene scaffolds containing the side chain of CQ have been reported to be potent antimalarials in the CQ-sensitive (HB3) and CQ-resistant (Dd2) strains.[16] Moreover derivatives of Schiff base hydrazones containing oxalamide functionality, various acrydinylhydrazones, and thiosemicarbazone having Fe(III) chelating activity have been reported as promising antimalarials.[17,18] The antioxidant phenolic compounds extracted from stem barks of *Parkia biglobosa* elicited significant antiplasmodial activity against the rodent malaria parasite.[19] We took 2-isopropyl-5-methylphenol, a naturally occurring phenolic antioxidant, as the core pharmacophoric unit which exhibited various pharmacological activities including antimicrobial,[20] antifungal,[21] radical scavenging,[22] and anti-inflammatory properties.[23] We optimized the scaffold with further chemical modification to derive a new class of Fe^{III}-PPIX binder with high affinity.

Our primary aim was to develop a new synthetic compound that would be effective against CQ-resistant and multi-drug-resistant strains. In this article, we report the synthesis of a new chemotype which prevents Hz formation by inhibiting free Fe^{III}-PPIX crystallization in FV in the malaria parasite. Aiming at heme detoxification procedure as a drug target, we engineered a class of bioactive compounds that exhibit antimalarial efficacy against CQ-sensitive (3D7) and -resistant (K1) strains of *P. falciparum* in vitro and also in vivo against multi-drug-resistant (MDR) parasites in the mouse model.

■ RESULTS AND DISCUSSION

Synthesis of Hydrazone Scaffolds (1−26). We commenced our study using 2-isopropyl-5-methylphenol as a starting material for the synthesis of hydrazonophenol by the para-formylation of commercially available 2-isopropyl-5-methylphenol (**i**) followed by the reaction with aldehyde (**ii**) in the hydrazine library.

The aldehyde (**ii**, 1.12 mmol, 1 equiv) was suspended in anhydrous methanol (2 mL) and stirred to obtain a clear solution. Respective hydrazines (1.1 equiv) were added to the solution portionwise, and the reaction mixture was allowed to stir for 6−8 h at room temperature to obtain the desired product compound (**1−6, 15−26**) or at 0 °C (**7−14**) (Figure 1). Upon completion, the solvent was evaporated under reduced pressure and the crude reaction mixture was purified by silica gel column chromatography or by crystallization. The

structures of compounds **1−26** were confirmed by NMR (^{1}H and ^{13}C) and LC−MS analyses.

Identification of the High-Affinity Fe^{III}-PPIX Interacting Compound. The molecules that can bind Fe^{III}-PPIX may inhibit hemozoin formation and lead to parasite death. Thus, we assessed the interactions of all of the synthesized hydrazonophenols with Fe^{III}-PPIX in silico. Some of these molecules had significant Fe^{III}-PPIX binding (<−4 kcal mol^{-1}), and among them compound **18** had an efficient Fe^{III}-PPIX binding affinity with a binding energy of −5.50 kcal mol^{-1} (Table S1, Supporting Information). The purity of the compound was confirmed by HPLC and X-ray crystallography (CCDC no. 1589463) (Figure 2A,B; Table S2, Supporting Information). In silico studies indicated that compound **18** interacted with Fe^{III}-PPIX through nonbonding π−π interactions between two pairs of sp^2-hybridized N atoms and the pyrrole unit of the Fe^{III}-PPIX ring (Figure 2C,D). The binding property of the hydrazonophenols was further evaluated by differential spectroscopy.[24] The data indicated strong Fe^{III}-PPIX binding of lead molecule **18** with an equilibrium dissociation constant (K_d) of 33.06 ± 0.11 nM (Figure 2E). The nonbonding π−π interaction can be attributed to high binding energy. The position of electronegative nitrogen atoms present both in the heterocyclic ring and in the unsaturated carbon−nitrogen double bond contributed significantly to the π interactions. Now, we were interested to find the chemical motif responsible for such strong Fe^{III}-PPIX binding of compound **18**.

Identification of the Fe^{III}-PPIX Binding Motif of Compound 18. In order to find out which moiety is responsible for Fe^{III}-PPIX binding, we trisected molecule **18** into three parts and evaluated the Fe^{III}-PPIX binding capacity by differential spectroscopy using individual segments. Compound **18** expectedly showed concentration-dependent Fe^{III}-PPIX binding (Figure 3A), in contrast, the three parts {the phenol (Figure 3B), the phenolic aldehyde (Figure 3C), and the hydrazine (Figure 3D)} did not exhibit any significant Fe^{III}-PPIX interactions. The study reflected that each phenol, aldehyde, and hydrazine scaffold showed incompetent Fe^{III}-PPIX binding, but the hybridized molecule, the hydrazonophenol (**18**), showed proficient binding with the macromolecule, Fe^{III}-PPIX. Thus, it can be concluded that the −C═N−NH− moiety in compound **18** was primarily required for binding. Next, we assessed the antiplasmodial activity of compounds in order to correlate with Fe^{III}-PPIX binding.
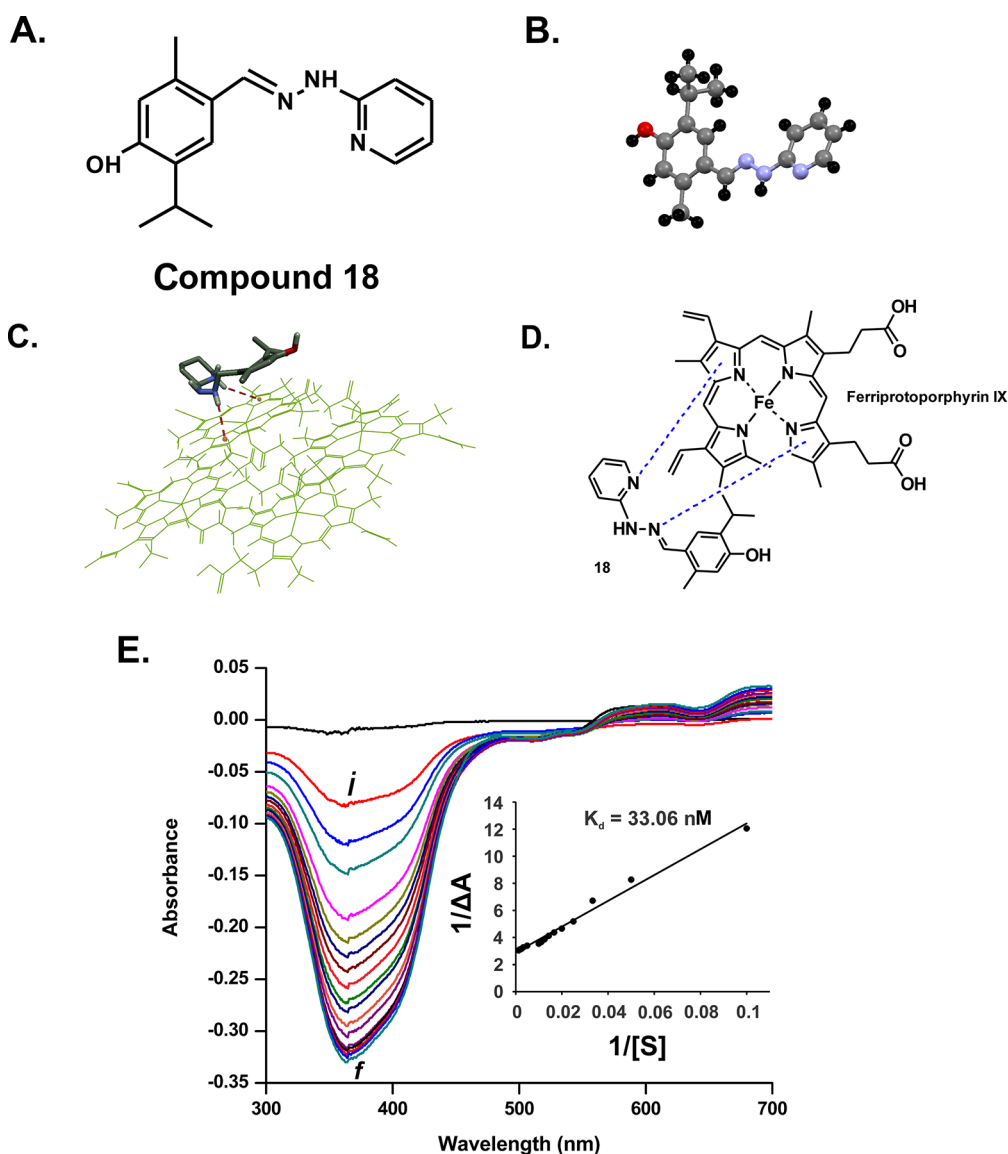
Figure 2. In silico analysis of the interaction between compound **18** and Fe^{III}-PPIX. (A) Compound **18**. (B) X-ray crystallographic structure of compound **18**. (C) Graphical representation of the probable mode of binding of compound **18** to hematin ($(Fe^{III}\text{-PPIX})_2$ $\pi-\pi$ dimer). The β-hematin tetramer was chosen as a representative unit for Hz. (D) Representative image for the binding of compound **18** with Fe^{III}-PPIX. (E) Binding of compound **18** with Fe^{III}-PPIX. The differential spectroscopic study was performed using compound **18** with increasing concentrations (10 nM to 800 nM; i, initial, 10 nM; f, final, 800 nM). The inset shows the $1/\Delta A$ versus $1/[S]$ plot that was used to calculate the dissociation constant (K_d) for the Fe^{III}-PPIX-**18** complex.

In Vitro Antiplasmodial Activity of Hydrazonophenols and SAR Studies. We screened the functionalized hydrazonophenols for their in vitro antimalarial activity against the CQ-sensitive (3D7) and -resistant (K1) strains of *P. falciparum* by the SYBR green assay.[25] The inhibitory concentration (IC_{50}) was quantitatively determined from the plot of compound concentrations against the percentage decrease in SYBR green fluorescence at respective concentrations compared to the DMSO control (Table 1). The pK_a and molecular polar surface areas (tPSA) were calculated using ChemBioDraw Ultra 14.0 (Table 1). Data indicated that primary scaffold 2-isopropyl-5-methylphenol (**i**) showed no significant antimalarial activity ($IC_{50} > 100$ μM) but that aldehyde (**ii**) and the derived simplest hydrazonophenol (**iii**) exerted a higher efficacy with an IC_{50} of around 63 μM against the sensitive strain. The most active scaffolds, **8** and **18**, were chosen for structure−activity relationship (SAR) analysis

(Figure 4). The study revealed that molecules with $n = 1$ and X, Y, Z = −CH (compounds **16** and **25**) were highly noneffective and that −CN and −CO₂H (electron-withdrawing functional groups) substitutions also did not show much improvement (compounds **6** and **21**). However, improved efficacy was found for $n = 0$ with X = N, Y, Z = H (compound **18**), and high pK_a values comparable to that of CQ. When Y and/or Z = N, the efficacy of the compounds was diminished or absent (compounds **17** and **19**). Besides, when $n = 0$ and X, Y, Z = −CH, highly electronegative group substitution (R = 4-F-3-Cl (**12**); 3,5-di-CF₃ (**14**); 1,2,3,4,5-penta-F (**8**)) was found to be effective against parasites, and the compounds had high $c \log P$ values with increased hydrophilicity. Compounds with fluorine substitution mainly at the ortho and para positions showed a greater degree of efficacy against *P. falciparum* strains (Table 1, entries 7, 9, and 12). Among them, the pentafluoro derivative, compound **8**,
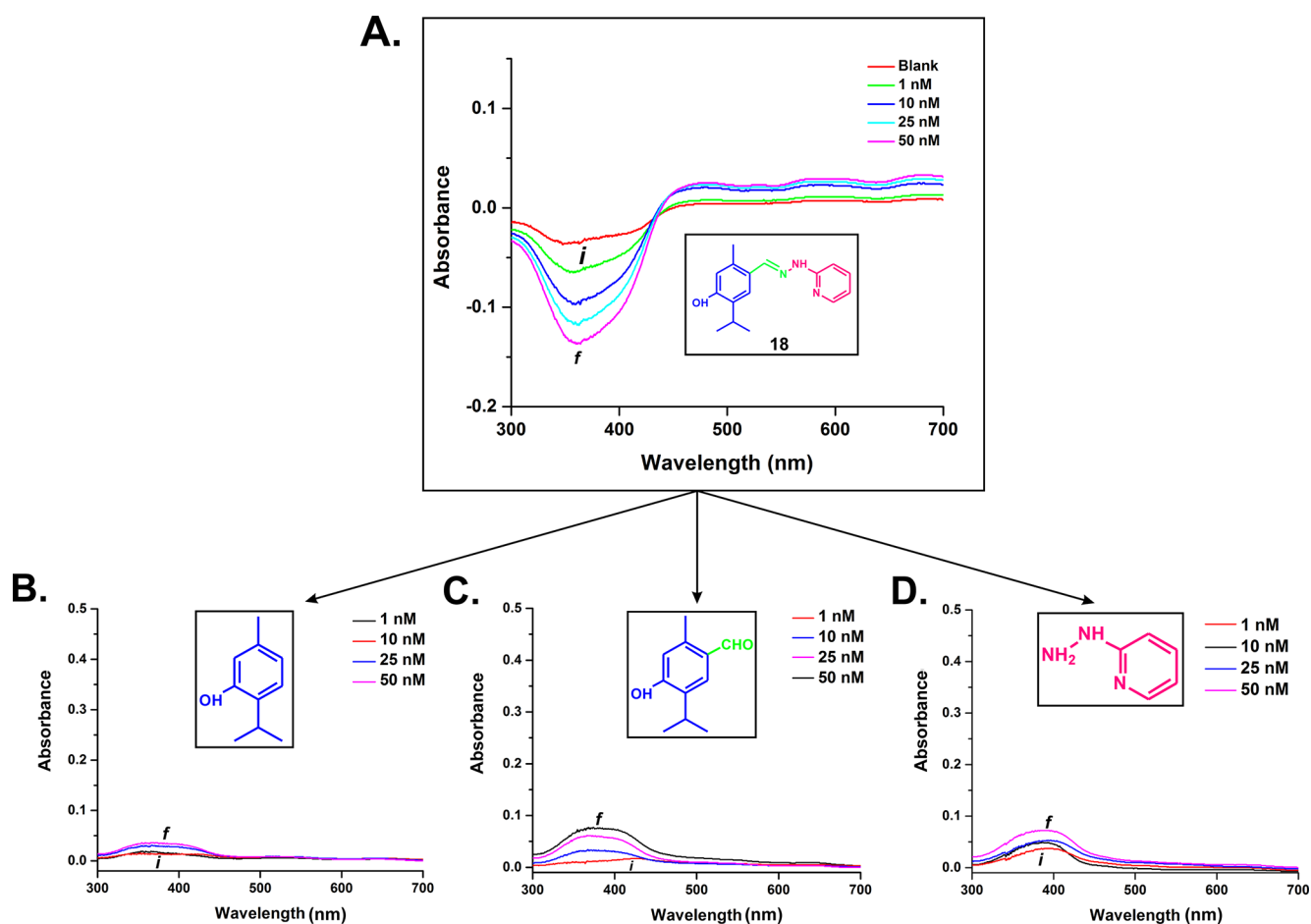
Figure 3. Identification of the Fe^{III}-PPIX binding motif of compound **18**. Binding analysis of different structural components of compound **18** with Fe^{III}-PPIX. (A) Compound **18**. (B) Phenolic scaffold. (C) Phenolic aldehyde moiety. (D) 2-Phenyl hydrazine. All compounds were used at increasing concentrations (1 to 50 nM; i, initial, 1 nM; f, final, 50 nM) with a fixed concentration of Fe^{III}-PPIX (5 μM).

had a relatively lower IC$_{50}$ (2.10 ± 0.27 μM) against the 3D7 strain of *P. falciparum*. Interestingly, the incorporation of the heterocyclic moiety in the hydrazine counterpart resulted in an increase in antiparasitic activity (Table 1, entries **15**, **18**, **19**, and**26**). Although compound **15** exhibited antiplasmodial activity against the CQ-sensitive 3D7 strain at low concentration, the diminished efficacy of compound **15** against the CQ-resistant K1 strain might be attributed to the reduced uptake or efflux of the molecule. Compound **18** containing the 2-pyridyl moiety had the highest antiplasmodial activity against CQ-sensitive 3D7 (IC$_{50}$ = 1.49 ± 0.16 μM) and CQ-resistant K1 (IC$_{50}$ = 2.56 ± 0.85 μM) strains. Compound **19** with nitrogen atom substitution at the para position of the ring showed decreased activity. However, the replacement of the pyridine moiety with a pyrimidine moiety (compound **20**) resulted in the loss of the antimalarial activity of the respective hydrazonophenol.

The SAR study delineated the role of the −C═N−NH− moiety in Fe^{III}-PPIX binding, which was thereby correlated with the antiplasmodial efficacy of hydrazonophenols. The calculated tPSA values (Table 1) pointed toward the high probability of the compounds permeating the cell-membrane. Compounds **8** or **18** had similar activities against the 3D7 strain. However, the advantage of compound **18** with respect to compound **8** was that the compound **18** exhibited similar behavior in sensitive and resistant strains of the parasite. It was evident that the structure of compound **18** provided a good

spatial advantage for a suitable nonbonding weak π-interaction between compound **18** and the two pyrrole moieties, as was deduced by the in silico study. The participation of 2-pyridine might stabilize the protonated form of compound **18**, probably through an intramolecular hydrogen bond. Previous studies showed that drug molecules with a planar conformation form a heme−drug complex through weak π−π interactions.[26−28] The absence of the nitrogen atom in the structural analogue of **18** resulted in the disappearance of interactions with the Fe^{III}-PPIX unit, which supported the experimental findings (Figures S1 and S2, Supporting Information). It depicted the positional significance of nitrogen atom in the heterocyclic ring. The data showed a moderate correlation between the dissociation constant (K_d) for the Fe^{III}-PPIX binding of hydrazonophenol with in vitro antiplasmodial activity (Table S3, Supporting Information). Moreover, because of the high pK_a of compound **18** (Table 1), it may be accumulated inside an acidic FV such as CQ.[29] Therefore, we were interested to trace the cellular localization of compound **18** in *P. falciparum*.

Cellular Localization of Fluorophore-Tagged Compound 18. To locate compound **18** inside the parasite, we designed and synthesized a fluorophore-tagged version of **18**, compound **28** (Figure 5A). Uranine, a well-known fluorophore, was coupled with compound **18** via an EDC-mediated coupling reaction.[30] Parasite culture was incubated with LysoTracker (to stain FV) and Hoechst 33342 (to stain the nucleus).[31] A set of noninfected RBCs incubated with

Table 1. In Vitro Screening of Antimalarial Activity of Compounds 1−26

Entry	—R	IC$_{50}$ (µM) Mean ± SEM[a] 3D7 strain	IC$_{50}$ (µM) Mean ± SEM[a] K1 strain	tPSA[b]	pKa	Entry	—R	IC$_{50}$ (µM) Mean ± SEM[a] 3D7 strain	IC$_{50}$ (µM) Mean ± SEM[a] K1 strain	tPSA[b]	pKa
1	2-Br-phenyl	>100	NA	44.62	9.09	14	3,5-(CF$_3$)$_2$-phenyl	>100	>100	44.62	9.91
2	3-Br-phenyl	59.66 ± 3.42	>100	44.62	9.91	15	4,5-dihydroimidazol-2-yl	3.46 ± 0.14	>100	69.01	9.87
3	4-Br-phenyl	25.11 ± 0.17	NA	44.62	9.91	16	benzoyl	33.55 ± 1.93	NA	61.69	9.86
4	3-Cl-phenyl	>100	>100	44.62	9.91	17	pyridine-2-carbonyl	>100	>100	74.05	9.86
5	4-Cl-phenyl	>100	NA	44.62	9.91	18	pyridin-2-yl	**1.49 ± 0.15**	**2.56 ± 0.85**	**56.98**	**9.89**
6	4-CN-phenyl	>100	26.53 ± 0.66	67.48	9.90	19	pyridin-4-yl	12.30 ± 0.17	10.55 ± 0.39	56.98	9.90
7	2,6-F$_2$-phenyl	3.07 ± 0.12	10.17 ± 0.04	44.62	9.91	20	pyrimidin-2-yl	NA	NA	69.34	9.88
8	pentafluorophenyl	2.10 ± 0.27	14.88 ± 0.83	44.62	9.91	21	4-COOH-phenyl	41.68 ± 3.10	73.94 ± 8.21	81.92	9.90
9	2,4-F$_2$-phenyl	6.96 ± 0.60	10.64 ± 0.11	44.62	9.92	22	N,N-dibenzylamino	28.93 ± 4.63	24.76 ± 0.70	35.83	9.85
10	3,5-F$_2$-phenyl	>100	42.99 ± 0.40	44.62	9.91	23	benzyloxycarbonyl	25.26 ± 2.87	24.54 ± 0.06	70.92	9.85
11	2,3,5,6-F$_4$-phenyl	10.77 ± 0.97	12.88 ± 0.17	44.62	9.91	24	N,N-diphenylamino	>100	NA	69.97	9.72
12	2-Cl-4-F-phenyl	2.17 ± 0.21	11.84 ± 0.09	44.62	9.91	25	4-OH-benzoyl	50.45 ± 3.34	>100	81.92	9.87
13	2,6-Cl$_2$-4-CF$_3$-phenyl	>100	>100	44.62	9.89	26	benzothiazol-2-yl	38.16 ± 6.53	31.29 ± 0.81	56.98	9.83
						iii	—NHNH$_2$	63.13 ± 5.21	n.d.	58.61	10.05

[a]In vitro antimalarial activity was presented as the IC$_{50}$ (mean ± SEM, wherever applicable), and values were the average of at least two independent assays carried out in triplicate. Compounds were incubated with parasites for 48 h. [b]tPSA and pK$_a$ values were calculated using ChemBioDraw Ultra 14.0. NA: not active. n.d.: not determined.
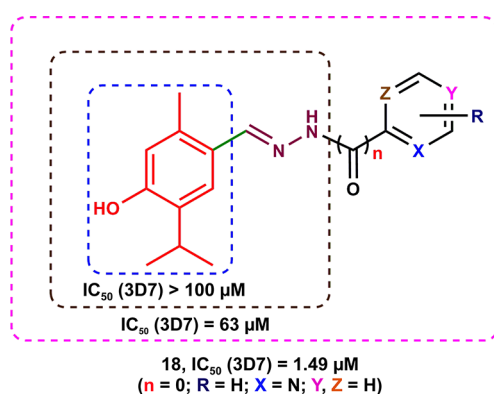
Figure 4. SAR studies for antiplasmodial efficacy of functionalized hydrazonophenols.

compound **28** was used as a control. The very selective uptake of compound **28** was evident from its colocalization with LysoTracker Red, which was localized specifically in parasite FV, near Hz, the black pigment found only in the FV of

parasitized RBCs (Figure 5B). SYBR green assay with compound **28** indicated no significant alteration of the antiplasmodial activity of compound **18** after fluorophore tagging (IC$_{50,\ 3D7}$ = 1.50 ± 0.06 µM; IC$_{50,\ K1}$ = 2.59 ± 0.02 µM).

Live-cell confocal imaging was done to track the intracellular entrapment of the molecule. As observed earlier, the hydrazone moiety and the nitrogen atom (in a heterocyclic ring) were essential to free heme binding, and the confocal imaging study is now corroborated with the phenomenon. The merge 3 segment confirmed the colocalization of fluorophore-tagged compound **18** (compound **28**) with LysoTracker, a dye that accumulates inside FV, the acidic organelle of the parasite (Figure 5B). The biochemical reason behind this might be the high pK$_a$ (∼8) of compound **28** that caused its entrapment inside the FV. The distributed pattern of LysoTracker and compound **28** might be due to the disruption of FV because of the accumulation of free Fe^{III}-PPIX that damaged FV. However, the leakage of FV might occur upon illumination of a live parasite under the microscope.[32]
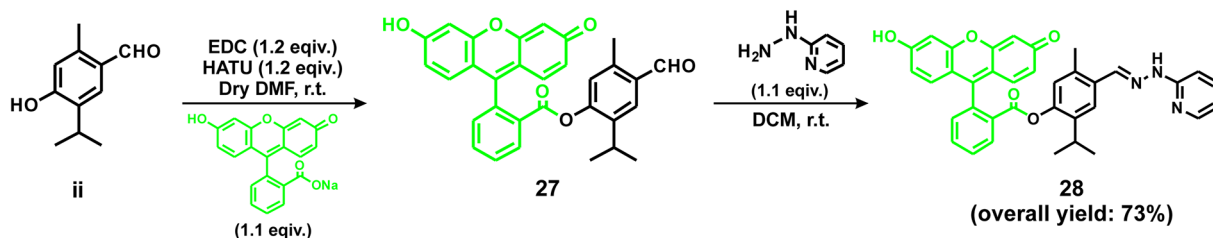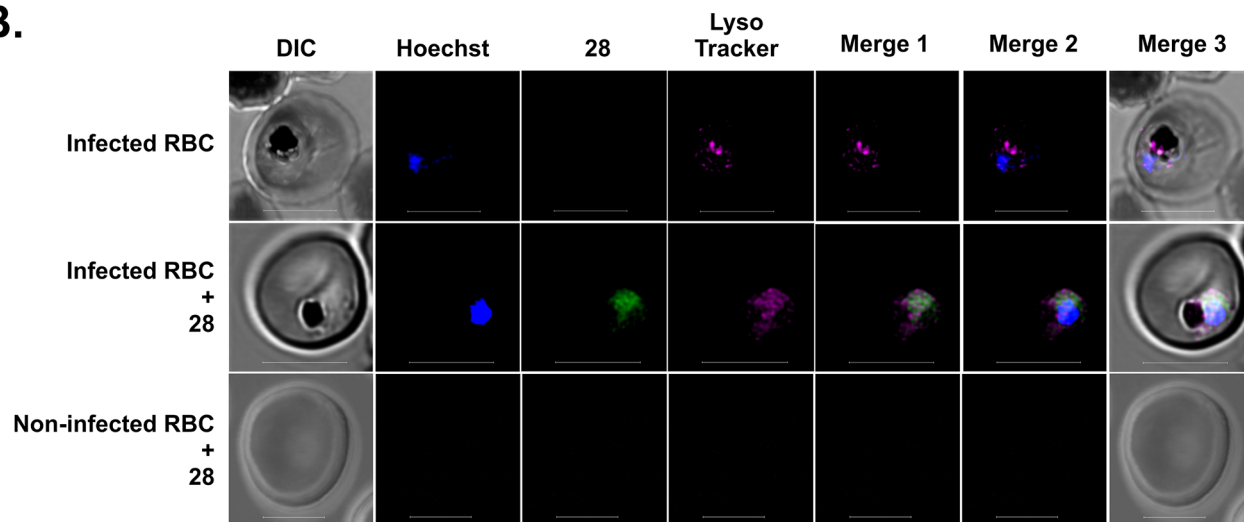
Figure 5. Confocal imaging of fluorophore-labeled compound **18** (compound **28**). (A) Addition of fluorophore signature to compound **18** through the two-step synthesis of oxygen-coupled ester via DCC coupling. (B) Live cell imaging of *P. falciparum* 3D7 cells after incubation with compound **28** (fluorophore-tagged **18**, green color, 5 μM), LysoTracker (magenta color), and Hoescht 33342 (blue color). The scale bar measures 5 μm. Merge 1: LysoTracker + **28**. Merge 2: LysoTracker + **28** + Hoescht. Merge 3: LysoTracker + **28** + Hoescht + differential interference contrast (DIC).

Restriction of Fe^{III}-PPIX Crystallization (Hemozoin) by Compound 18. The localization of the fluorophore-tagged version of compound **18** in the acidic vacuole of the parasite prompted us to investigate its effect on the free heme detoxification system in FV. The parasite was exposed to compound **18** at different concentrations, and the outcome was evaluated in terms of the change in pH of the FV using a LysoSensor Green acidotropic probe. The treated parasites were incubated with LysoSensor Green, and the fluorescence intensity was measured. A gradual decrease in fluorescence intensity with increasing concentrations (10−100 μM) of compound **18** indicated the change in the pH of FV due to the basic nature of the compound (Figure 6A). Next, we incubated the parasite with compound **18** and measured the Hz content inside the parasite to follow the effect on hemozoin formation. The data clearly indicated that compound **18** concentration-dependently inhibited Hz formation in *P. falciparum* (Figure 6B). DMSO was used as a vehicle control. The stability of compound **18** was also assessed at a food vacuolar pH of 5.2 as well as at a physiological pH of 7.4 by mass spectrometry. This compound was found to be stable at both pH values (Figure S3, Supporting Information). The inhibitory effect of the compound in vitro on heme crystallization was further confirmed by following the inhibition of parasite-lysate-mediated Hz formation at pH 5.2;[33] a cell-free system was established by mimicking conditions such as those for FV. The data showed that compound **18** concentration-dependently inhibited heme crystallization (Figure 6C). Moreover, the

accumulation of free Fe^{III}-PPIX in solution as a consequence of the inhibition of Hz formation by compound **18** was also measured as described.[34] Compound **18** concentration-dependently inhibited Fe^{III}-PPIX crystallization, thereby leading to free Fe^{III}-PPIX accumulation (Figure 6C).

LysoSensor Green is a pH-sensitive fluorescent probe and gets accumulated in acidic compartments where it becomes fluorescent upon protonation. The fluorescence intensity exerted by this probe increases with the lowering of the pH of the solution. A gradual decrease in fluorescence intensity with increasing concentration of compound **18** indicated a relative elevation of the pH of the acidic organelle (Figure 6A). This phenomenon can be attributed to the high pK_a value of the compound. One of the major functions of FV in parasites is the detoxification of pro-oxidant and toxic-free Fe^{III}-PPIX formed after hemoglobin digestion by converting it into an inert polymer Hz, and the food vacuolar localization of compound **18** indicated its capability to affect the free heme detoxification process.

Arrest of Intraerythrocytic Stage Progression of *P. falciparum*. In vitro inhibition of Hz formation and its impact on parasite growth were further validated by microscopic studies. To follow the progression of stages of parasites in the presence of compound **18**, we treated the synchronized ring stage of *P. falciparum* 3D7 with the compound. The morphology of the parasite along with the percentage of parasitemia was assessed at an interval of 10 h. A microscopic view identified the pyknotic morphology of the parasite after
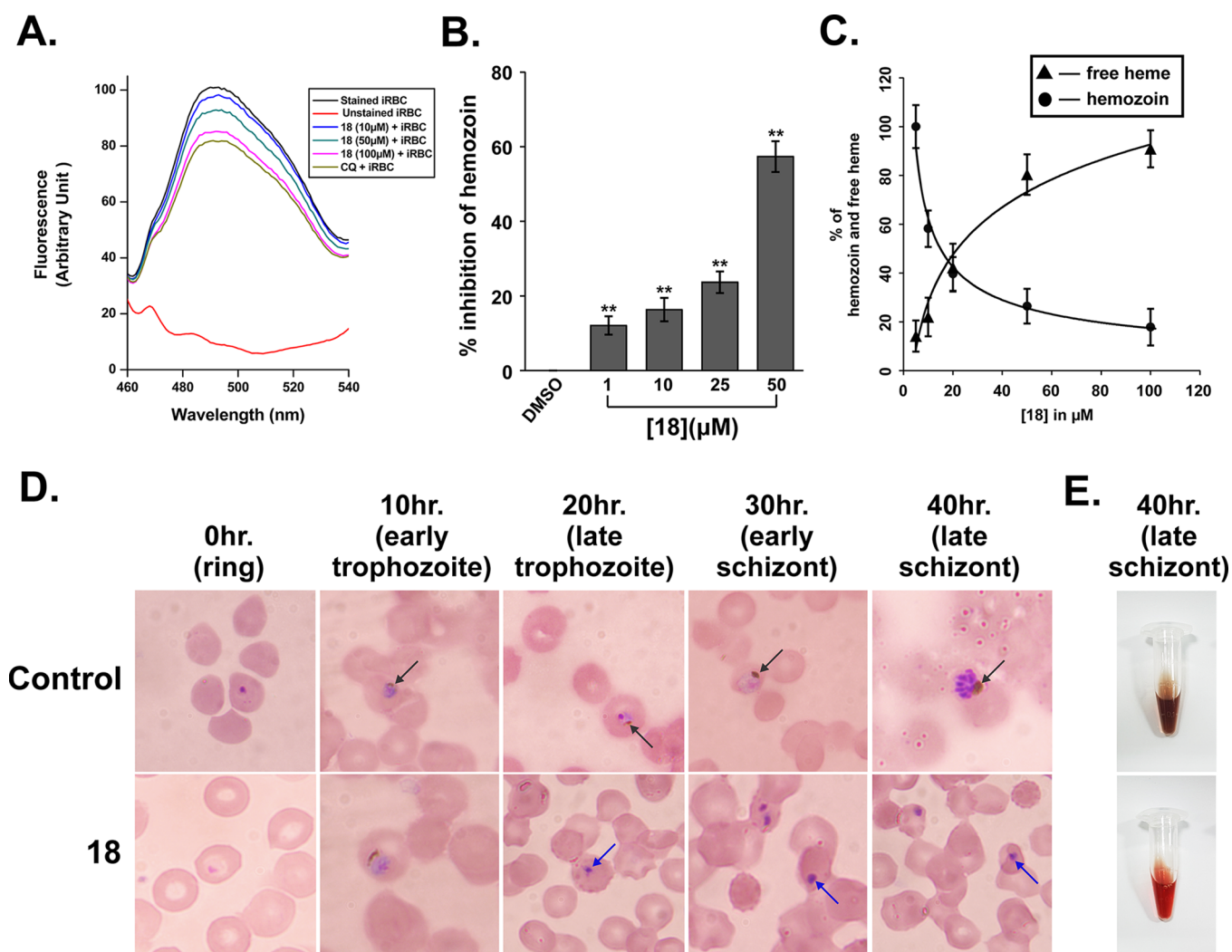
Figure 6. Effect of compound **18** on the pH of parasite food vacuole (FV) and hemozoin formation. (A) Change in the pH of parasite FV in the presence of compound **18** (10−100 μM) as measured by LysoSensor Green DND-189. iRBC: infected RBC; CQ was used as a positive control. (B) Inhibition of Hz formation in *P. falciparum* by compound **18** (1−50 μM) in culture. Data represent the mean ± SEM. Data were collected from at least two independent experiments (**, $P \leq 0.01$ compared to control). (C) Inhibition of parasite lysate-mediated Hz formation and quantification of free Fe^{III}-PPIX in the presence of compound **18** (5−100 μM). Data represent the mean ± SEM (D) Microscopic images of *P. falciparum* treated with compound **18** (5 μM) and DMSO (vehicle control). The black arrow indicates the Hz formed inside a healthy parasite, and the blue arrow indicates the dead parasite. (E) Visualization of the Hz of parasite lysate collected from the control and treated (40 h) parasite.

20 h of treatment with compound **18**. The compound inhibited parasite growth and resulted in its death, as was evident from its abnormal morphology. After 40 h, an untreated parasite grew to become schizont while compound **18** treatment resulted in parasite death marked by the single blue spots (Figure 6D). After 40 h of treatment, a very small amount of Hz was present in treated parasite lysate compared to amount in the untreated set. This confirmed that compound **18** effectively killed the parasite whereas parasites in the control set were able to grow and form Hz. The untreated lysate was red in color while the treated lysate was found to be dark in color due to the presence of excess Hz (Figure 6E). The irregular and abnormal shape of the parasite nucleus was detected under the microscope. The inhibition of Hz crystallization in the presence of compound **18** causes the accumulation of free heme, which in turn generates an oxidative insult to the parasite, leading to death.

Nonpromiscuous Nature of Compound 18. Compound **18** was assessed for its selectivity of action and cellular toxicity.

Keeping in mind the potential safety issues of pan-assay interference compounds (PAINs) in the arena of anti-infective drug innovation, we performed assays with several nonrelated drug targets.[35] Still, even with its promiscuous nature, compounds with exceptional effectiveness should be cogitated for the invention of new therapeutic.[36] We followed Soret spectroscopy of hemoglobin (Hb) at a physiological pH of 7.4 in the presence of increasing concentrations of compound **18** to follow the interaction of the compound with the heme (Fe^{II}-PPIX) present in hemoglobin. Data showed no change in the absorbance maxima of Hb, which indicated that compound **18** did not interact with the Fe^{II}-PPIX of hemoglobin (Figure 7A). The data also confirmed the specific interaction of compound **18** only with Fe^{III}-PPIX but not with Fe^{II}-PPIX in Hb. The hemolytic activity of compound **18** (100 μM) was also studied. Compound **18** did not exhibit any significant hemolytic activity when it was incubated with human RBC for 12 h (Figure 7B). Saponin (0.05%), which causes the lysis of RBC, was used as a positive control. The nonpromiscuous nature of
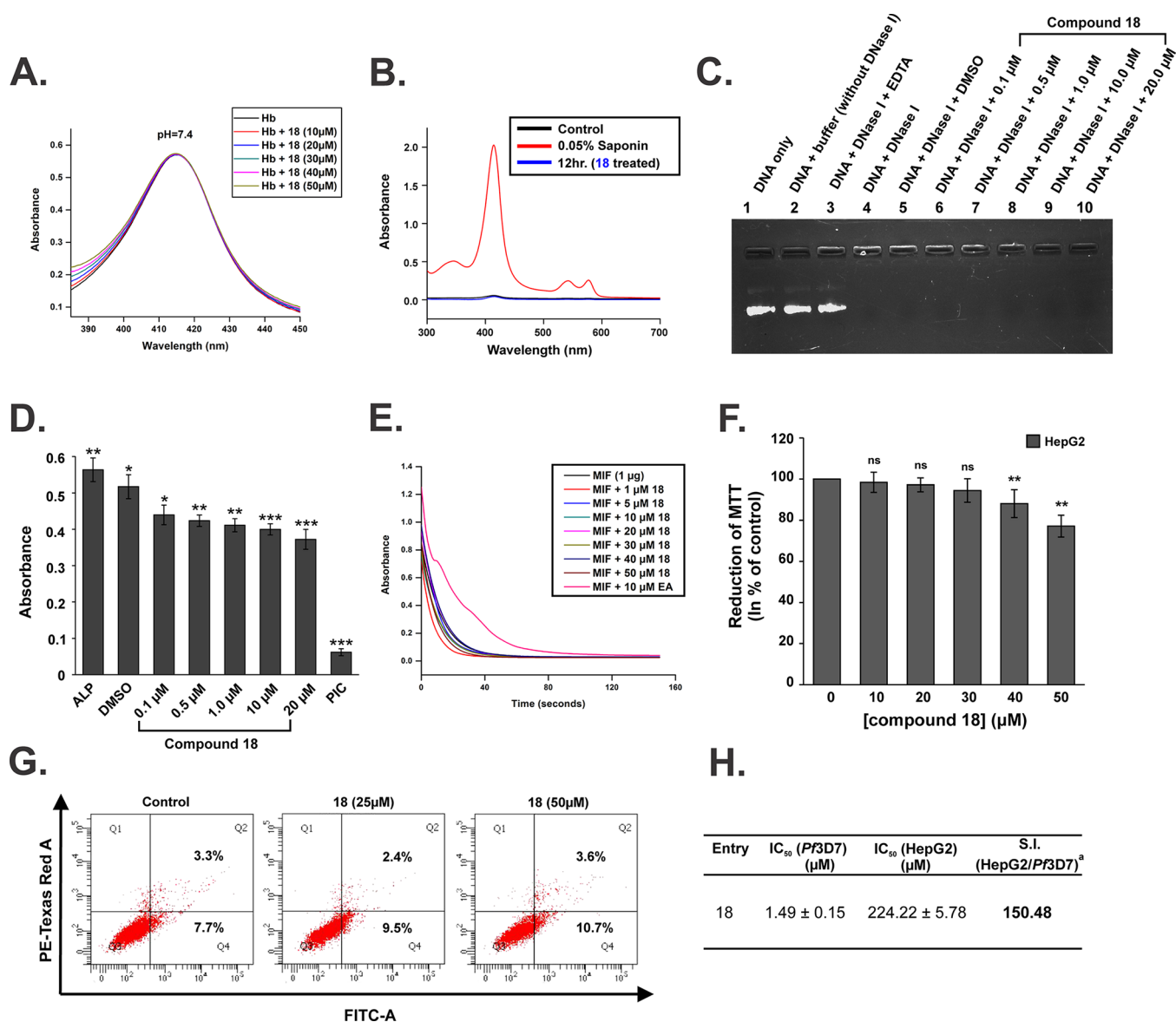
Figure 7. Evaluation of the nonpromiscuous nature of compound **18**. (A) Interaction of compound **18** with hemoglobin (Hb). The compound did not bind to Hb (pH 7.4), and Hb spectra were recorded with increasing concentrations (10−50 μM) of compound **18**. (B) Nonhemolytic property of compound **18**. Soret spectra were recorded from the supernatant of RBCs exposed to compound **18** (100 μM) for 12 h. Saponin (0.05%) was used as positive control. (C) Effect of compound **18** on DNase I activity; compound **18** (0.1−20 μM) was incubated with DNA and DNase I. Experimental sets were described along with the lane number of agarose gel. EDTA (20 mM) was used as a positive control, and DMSO was used as a control blank. (D) Effect of compound **18** (0.1−20 μM) on alkaline phosphatase activity. Phosphatase inhibitory cocktail (PIC) was used as a positive control. Data represent the mean ± SEM {*$P \leq 0.05$, **$P \leq 0.01$, ***$P \leq 0.001$; ns, not significant ($P > 0.05$)}. (E) MIF tautomerase activity with increasing concentrations (1−50 μM) of compound **18**. Ellagic acid (10 μM) was used as a positive control. (F) MTT reduction assay to follow the effect of compound **18** on cell viability. The experiment was performed in triplicate. Data represent the mean ± SEM {(**$P \leq 0.01$; ns, not significant ($P > 0.05$)}. (G) FACS analysis to study HepG2 cell death in the presence of different concentrations (10−50 μM) of compound **18**. Each value in the Q2 or Q4 quadrant depicts the percentage of cells showing late apoptotic−necrotic or apoptotic cell death, respectively. Dot-plot representations of FACS analysis are representative of a single experiment out of the independent experiments performed in triplicate. (H) Selectivity index (S.I.) of compound **18**. Details of the methodology are described in the Materials and Methods section in the Supporting Information.

compound **18** was further verified by assessing its effects on nonrelated proteins and the cell system. Therefore, DNase I, alkaline phosphatase (ALP), and macrophage migration inhibitory factor (MIF) tautomerase activities in the presence of compound **18** were examined. The inhibitory activity of compound **18** against DNase I was checked using a plasmid DNA (pBR322). Data showed that DNase I completely cleaved plasmid DNA alone and in the presence of compound **18** (0.1−20 μM), indicating that compound **18** did not affect

the DNase I activity (Figure 7C). However, EDTA, which was used as a positive control, prevented the activity of DNase I (Figure 7C). The enzymatic activity of ALP (Figure 7D) and the tautomerase activity MIF (Figure 7E) also remained unaltered in the presence of different concentrations of compound **18**. A slight decrease in optical density in the set of positive controls of ALP may be attributed to the effect of DMSO. The effect of compound **18** on cell viability was assessed by the 3-(4,5-dimethylthiazol-2-yl)-2,5-diphenyltetra-

zolium bromide (MTT) reduction assay (Figure 7F). A negligible loss of cell viability was observed as there was not much alteration seen in the amount of purple-colored formazan formed due to the reduction of MTT by the functional dehydrogenases within the treated cells compared with the control set. This data was well supported by the results obtained from flow cytometric analysis (FACS), where insignificant apoptotic cell death was detected (Figure 7G).

The presence of an almost equal proportion of HepG2 cells in the Q4 quadrant (apoptotic compartment) revealed the minimal toxicity of compound 18. The negligible effect of the compound on the viability of the HepG2 cell was further evident from the MTT reduction assay, indicating a high IC_{50} value. The IC_{50} value was obtained from the plot of the percentage of viable cells against the concentration of treated compound. The intensity of formazan absorbance was directly proportional to the viable cell density. The assessment of the selectivity index using the mammalian HepG2 cell line indicated a high selectivity index (S.I. = 150.48) for the compound (Figure 7H). Thus, the data obtained from these experiments established the nonpromiscuous nature and insignificant cellular toxicity of compound 18.

In Vivo Antimalarial Activity of Compound 18 against *P. yoelii* and *P. berghei* ANKA. In Peter's four day test, Swiss albino mice infected with lethal strains were treated with compound 18 intraperitoneally once a day for four subsequent days, commencing 4 h after the administration of parasitized erythrocytes intraperitoneally. Mice were treated with compound 18 in doses of 25, 50, 75, and 100 mg kg^{-1} body weight wherein each experimental set contained five mice. DMSO (vehicle) and antimalarial drug α/β-arteether were taken as the control and the positive control, respectively. The suppression of the percentage of parasitemia clearly indicated the antimalarial efficacy of compound 18 at a dose of 100 mg kg^{-1}, which showed 100% suppression of parasitemia on day 5 with mean survival days (MSDs) of 15.2 for the animals (Table 2). There was a significant drop in the parasite load in the 100 mg kg^{-1} treatment set, which was almost comparable to α/β-arteether. Compound 18 showed almost complete suppression of the parasitemia in vivo and exerted improved survival rates with increasing doses (Table 2 and Figure 8). Only two doses (50 and 100 mg kg^{-1}) of compound 18 were selected to check the efficacy in the mice infected with *P. berghei* ANKA that causes cerebral malaria.[37] The activity of 18 against *P. berghei* was found to be similar to that of *P. yoelii*, indicating the efficacy and broad spectrum antimalarial activity of 18 against multiple species of *Plasmodium*. The drug likelihood of compound 18 was measured in silico using Lipinski's rule of five (Table S4, Supporting Information).

The decrease in the parasitemia in animals showed the in vivo efficacy of the molecule. Moreover, the molecule was found to be active against different species of *P. falciparum*. However, the recurrence of parasitemia in mice that caused death after day 15 might be due to low bioavailability, low membrane permeability, or the difference in efficacy of compound 18 against human and rodent malaria parasites.

■ CONCLUSIONS

Compound 18, a nanomolar binder of ferriprotoporphyrin IX (heme), was developed by rational structure-based design, which inhibited hemozoin formation targeting the food vacuole of *P. falciparum* and offered antimalarial activity against the drug-resistant parasite in vitro and in vivo. The

Table 2. Peter's Four-Day Test for Parasitemia Suppression by Compound 18

compound	dose (mg kg^{-1})	parasitemia suppression (%)[a]	MSD[b]	survival[c]
control	0.0 (*P. yoelii*)	0.0	4.3	0/5
	0.0 (*P. berghei*)	0.0	4.0	0/5
α/β arteether	4 × 25 (*P. yoelii*)	100.0	n.d.	5/5
	4 × 25 (*P. berghei*)	100.0	n.d.	5/5
compound 18	4 × 25 (*P. yoelii*)	59.0	7.8	0/5
	4 × 25 (*P. berghei*)	n.d.	n.d.	-
	4 × 50 (*P. yoelii*)	78.1	10.6	1/5
	4 × 50 (*P. berghei*)	79.8	11.8	1/5
	4 × 75 (*P. yoelii*)	81.8	12.4	3/5
	4 × 75 (*P. berghei*)	n.d.	n.d.	
	4 × 100 (*P. yoelii*)	100.0	15.2	4/5
	4 × 100 (*P. berghei*)	97.5	16.6	3/5

[a]Parasitemia was determined on the fifth day after the completion of treatment. Percent parasitemia suppression was calculated as follows: $[(C - P)/C] \times 100$, where C is the parasitemia in the control group and P is the parasitemia in the treated group. [b]Mean survival time in days (MSD). [c]Number of healthy mice on day 15. n.d.: not determined.
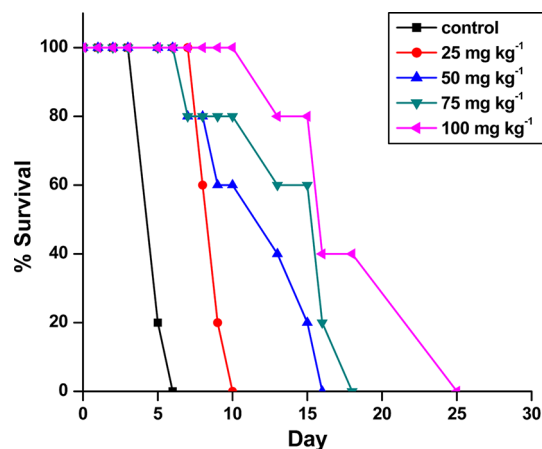
Figure 8. Compound 18 increases the survival rate of mice infected with the MDR strain (*P. yoelii*). Percentage survival of mice treated with different doses (0−100 mg kg^{-1} body weight) of compound 18 followed through the days after infection. Vehicle-treated mice were taken as the control. Five animals were used for each set of doses. Mice were euthanized when parasitemia reached 60% in order to avoid death otherwise.

efficacy of the compound against different *Plasmodium* species further indicated the potential activity of the compound against other species that cause malaria in humans. The activity of the compound at micromolar concentration in in vitro experiments might be due to its low solubility or permeability; however, the target of the molecule was validated by confirmatory experiments. The scope of this article was the synthesis and validation of an active pharmacophore against malaria. The active pharmacophore that was identified needs further

optimization of the chemical scaffold, which may improve its antimalarial activity and bioavailability. Thus, compound **18** represented a new antimalarial chemotype against resistant malaria.

■ MATERIALS AND METHODS

Materials and methods are described elaborately in the associated Supporting Information.

■ ETHICS STATEMENT

All mice were received from the animal house of CSIR-Indian Institute of Chemical Biology, Kolkata, India. We strictly followed procedures for handling animal and experiments in compliance with the regulations of the Institutional Animal Ethics Committee (IAEC) and the Committee for the Purpose of Control and Supervision of Experiments on Animals (CPCSEA, permit number 147/1999/CPCSEA).

■ ASSOCIATED CONTENT

Ⓢ Supporting Information

The Supporting Information is available free of charge on the ACS Publications website at DOI: 10.1021/acsinfec-dis.8b00178.

> General information, analysis of Fe^{III}-PPIX binding with hydrazonophenols, single-crystal X-ray structure of compound **18**, macromolecular interaction study of structural analogues of compound **18**, correlation between IC$_{50}$ and the equilibrium dissociation constant, stability of compound **18**, stability of compound **18** at food vacuolar low pH, evaluation of ADME properties, materials and methods, analytical data, and ^{1}H and ^{13}C NMR spectra for compounds **ii**, **1−20**, **27**, and **28** (PDF)

■ AUTHOR INFORMATION

Corresponding Author

*E-mail: ubandyo_1964@yahoo.com, udayb@iicb.res.in. Tel: 91-33-24995735. Fax: 91-33-4730284.

ORCID Ⓘ

Shubhra Jyoti Saha: 0000-0001-6536-6060
Asim Azhar Siddiqui: 0000-0002-0860-1535
Debanjan Saha: 0000-0002-8311-530X
Uday Bandyopadhyay: 0000-0002-5928-6790

Notes

The authors declare no competing financial interest.

■ ACKNOWLEDGMENTS

■ REFERENCES

(1) WHO. *World Malaria Report 2016*; 2017.

(2) Davis, T. M. E., Hung, T.-Y., Sim, I.-K., Karunajeewa, H. A., and Ilett, K. F. (2005) Piperaquine: A Resurgent Antimalarial Drug. *Drugs* 65 (1), 75−87.

(3) WHO. *World Malaria Report 2017*; 2018.

(4) Lu, F., Culleton, R., Zhang, M., Ramaprasad, A., von Seidlein, L., Zhou, H., Zhu, G., Tang, J., Liu, Y., Wang, W., Cao, Y., Xu, S., Gu, Y., Li, J., Zhang, C., Gao, Q., Menard, D., Pain, A., Yang, H., Zhang, Q., and Cao, J. (2017) Emergence of Indigenous Artemisinin-Resistant *Plasmodium Falciparum* in Africa. *N. Engl. J. Med.* 376 (10), 991−993.

(5) Lin, J. T., Juliano, J. J., and Wongsrichanalai, C. (2010) Drug-Resistant Malaria: The Era of ACT. *Curr. Infect. Dis. Rep.* 12 (3), 165−173.

(6) Verdier, F., Le Bras, J., Clavier, F., Hatin, I., and Blayo, M. C. (1985) Chloroquine Uptake by *Plasmodium Falciparum*-Infected Human Erythrocytes during in Vitro Culture and Its Relationship to Chloroquine Resistance. *Antimicrob. Agents Chemother.* 27 (4), 561−564.

(7) Fitch, C. D., Chevli, R., Banyal, H. S., Phillips, G., Pfaller, M. A., and Krogstad, D. J. (1982) Lysis of *Plasmodium Falciparum* by Ferriprotoporphyrin IX and a Chloroquine-Ferriprotoporphyrin IX Complex. *Antimicrob. Agents Chemother.* 21 (5), 819−822.

(8) Pal, C., Kundu, M. K., Bandyopadhyay, U., and Adhikari, S. (2011) Synthesis of Novel Heme-Interacting Acridone Derivatives to Prevent Free Heme-Mediated Protein Oxidation and Degradation. *Bioorg. Med. Chem. Lett.* 21 (12), 3563−3567.

(9) Pal, C., and Bandyopadhyay, U. (2012) Redox-Active Antiparasitic Drugs. *Antioxid. Redox Signaling* 17 (4), 555−582.

(10) Dey, S., Mazumder, S., Siddiqui, A. A., Iqbal, M. S., Banerjee, C., Sarkar, S., De, R., Goyal, M., Bindu, S., and Bandyopadhyay, U. (2014) Association of Heme Oxygenase 1 with the Restoration of Liver Function after Damage in Murine Malaria by *Plasmodium Yoelii*. *Infect. Immun.* 82 (8), 3113−3126.

(11) Egan, T. J., Mavuso, W. W., and Ncokazi, K. K. (2001) The Mechanism of β-Hematin Formation in Acetate Solution. Parallels between Hemozoin Formation and Biomineralization Processes. *Biochemistry* 40 (1), 204−213.

(12) Fitch, C. D., and Kanjananggulpan, P. (1987) The State of Ferriprotoporphyrin IX in Malaria Pigment. *J. Biol. Chem.* 262 (32), 15552−15555.

(13) Fidock, D. A., Nomura, T., Talley, A. K., Cooper, R. A., Dzekunov, S. M., Ferdig, M. T., Ursos, L. M. B., Sidhu, A. B. S., Naude, B., Deitsch, K. W., Su, X. Z., Wootton, J. C., Roepe, P. D., and Wellems, T. E. (2000) Mutations in the *P. Falciparum* Digestive Vacuole Transmembrane Protein *Pf*CRT and Evidence for Their Role in Chloroquine Resistance. *Mol. Cell* 6 (4), 861−871.

(14) Kappe, S. H. I., Vaughan, A. M., Boddey, J. A., and Cowman, A. F. (2010) That Was Then But This Is Now: Malaria Research in the Time of an Eradication Agenda. *Science (Washington, DC, U. S.)* 328 (5980), 862−866.

(15) Ocheskey, J. A., Harpstrite, S. E., Oksman, A., Goldberg, D. E., and Sharma, V. (2005) Metalloantimalarials: Synthesis and Characterization of a Novel Agent Possessing Activity against *Plasmodium Falciparum*. *Chem. Commun.* 0 (12), 1622.

(16) Harpstrite, S. E., Collins, S. D., Oksman, A., Goldberg, D. E., and Sharma, V. (2008) Synthesis, Characterization, and Antimalarial Activity of Novel Schiff-Base-Phenol and Naphthalene-Amine Ligands. *Med. Chem.* 4 (4), 392−395.

(17) Sharma, M., Chauhan, K., Srivastava, R. K., Singh, S. V., Srivastava, K., Saxena, J. K., Puri, S. K., and Chauhan, P. M. S. (2014) Design and Synthesis of a New Class of 4-Aminoquinolinyl- and 9-Anilinoacridinyl Schiff Base Hydrazones as Potent Antimalarial Agents. *Chem. Biol. Drug Des.* 84 (2), 175−181.

(18) Walcourt, A., Loyevsky, M., Lovejoy, D. B., Gordeuk, V. R., and Richardson, D. R. (2004) Novel Aroylhydrazone and Thiosemicarbazone Iron Chelators with Anti-Malarial Activity against Chloroquine-Resistant and -Sensitive Parasites. *Int. J. Biochem. Cell Biol.* 36 (3), 401−407.

(19) Builders, M., Alemika, T., and Aguiyi, J. (2014) Antimalarial Activity and Isolation of Phenolic Compound from Parkia Biglobosa. *IOSR J. Pharm. Biol. Sci. 9* (3), 78−85.

(20) Tepe, B., Daferera, D., Sökmen, M., Polissiou, M., and Sökmen, A. (2004) *In Vitro* Antimicrobial and Antioxidant Activities of the Essential Oils and Various Extracts of *Thymus Eigii* M. Zohary et P.H. Davis. *J. Agric. Food Chem. 52* (5), 1132−1137.

(21) Podobnik, B., Stojan, J., Lah, L., Kraševec, N., Seliškar, M., Rižner, T. L., Rozman, D., and Komel, R. (2008) CYP53A15 of Cochliobolus Lunatus, a Target for Natural Antifungal Compounds. *J. Med. Chem. 51* (12), 3480−3486.

(22) Aeschbach, R., Löliger, J., Scott, B. C., Murcia, A., Butler, J., Halliwell, B., and Aruoma, O. I. (1994) Antioxidant Actions of Thymol, Carvacrol, 6-Gingerol, Zingerone and Hydroxytyrosol. *Food Chem. Toxicol. 32* (1), 31−36.

(23) Braga, P. C., Dal Sasso, M., Culici, M., Bianchi, T., Bordoni, L., and Marabini, L. (2006) Anti-Inflammatory Activity of Thymol: Inhibitory Effect on the Release of Human Neutrophil Elastase. *Pharmacology 77* (3), 130−136.

(24) Ajdačić, V., Senerovic, L., Vranić, M., Pekmezovic, M., Arsic-Arsnijevic, V., Veselinovic, A., Veselinovic, J., Šolaja, B. A., Nikodinovic-Runic, J., and Opsenica, I. M. (2016) Synthesis and Evaluation of Thiophene-Based Guanylhydrazones (Iminoguanidines) Efficient against Panel of Voriconazole-Resistant Fungal Isolates. *Bioorg. Med. Chem. 24* (6), 1277−1291.

(25) Choubey, V., Guha, M., Maity, P., Kumar, S., Raghunandan, R., Maulik, P. R., Mitra, K., Halder, U. C., and Bandyopadhyay, U. (2006) Molecular Characterization and Localization of *Plasmodium Falciparum* Choline Kinase. *Biochim. Biophys. Acta, Gen. Subj. 1760* (7), 1027−1038.

(26) Wicht, K. J., Combrinck, J. M., Smith, P. J., Hunter, R., and Egan, T. J. (2016) Identification and SAR Evaluation of Hemozoin-Inhibiting Benzamides Active against *Plasmodium Falciparum*. *J. Med. Chem. 59* (13), 6512−30.

(27) Okombo, J., Singh, K., Mayoka, G., Ndubi, F., Barnard, L., Njogu, P. M., Njoroge, M., Gibhard, L., Brunschwig, C., Vargas, M., Keiser, J., Egan, T. J., and Chibale, K. (2017) Antischistosomal Activity of Pyrido[1,2-A]benzimidazole Derivatives and Correlation with Inhibition of β-Hematin Formation. *ACS Infect. Dis. 3* (6), 411−420.

(28) De Villiers, K. A., Gildenhuys, J., and Le Roex, T. (2012) Iron(III) Protoporphyrin IX Complexes of the Antimalarial Cinchona Alkaloids Quinine and Quinidine. *ACS Chem. Biol. 7* (4), 666−671.

(29) Yayon, A., Cabantchik, Z. I., and Ginsburg, H. (1984) Identification of the Acidic Compartment of *Plasmodium Falciparum*-Infected Human Erythrocytes as the Target of the Antimalarial Drug Chloroquine. *EMBO J. 3* (11), 2695−2700.

(30) Pal, C., Bindu, S., Dey, S., Alam, A., Goyal, M., Iqbal, M. S., Sarkar, S., Kumar, R., Halder, K. K., Debnath, M. C., Adhikari, S., and Bandyopadhyay, U. (2012) Tryptamine-Gallic Acid Hybrid Prevents Non-Steroidal Anti-Inflammatory Drug-Induced Gastropathy: Correction of Mitochondrial Dysfunction and Inhibition of Apoptosis in Gastric Mucosal Cells. *J. Biol. Chem. 287* (5), 3495−3509.

(31) Iqbal, M. S., Siddiqui, A. A., Banerjee, C., Nag, S., Mazumder, S., De, R., Saha, S. J., Karri, S. K., and Bandyopadhyay, U. (2018) Detection of Retromer Assembly in *Plasmodium Falciparum* by Immunosensing Coupled to Surface Plasmon Resonance. *Biochim. Biophys. Acta, Proteins Proteomics 1866*, 722.

(32) Wissing, F., Sanchez, C. P., Rohrbach, P., Ricken, S., and Lanzer, M. (2002) Illumination of the Malaria Parasite *Plasmodium Falciparum* Alters Intracellular pH. Implications for Live Cell Imaging. *J. Biol. Chem. 277* (40), 37747−37755.

(33) Ncokazi, K. K., and Egan, T. J. (2005) A Colorimetric High-Throughput β-Hematin Inhibition Screening Assay for Use in the Search for Antimalarial Compounds. *Anal. Biochem. 338* (2), 306−319.

(34) Fong, K. Y., Sandlin, R. D., and Wright, D. W. (2015) Identification of β-Hematin Inhibitors in the MMV Malaria Box. *Int. J. Parasitol.: Drugs Drug Resist. 5* (3), 84−91.

(35) Panaceas, I. M. (2017) The Ecstasy and Agony of Assay Interference Compounds. *ACS Cent. Sci. 3* (3), 143−147.

(36) Arrowsmith, C. H., Audia, J. E., Austin, C., Baell, J., Bennett, J., Blagg, J., Bountra, C., Brennan, P. E., Brown, P. J., Bunnage, M. E., Buser-Doepner, C., Campbell, R. M., Carter, A. J., Cohen, P., Copeland, R. A., Cravatt, B., Dahlin, J. L., Dhanak, D., Edwards, A. M., Frederiksen, M., Frye, S. V., Gray, N., Grimshaw, C. E., Hepworth, D., Howe, T., Huber, K. V., Jin, J., Knapp, S., Kotz, J. D., Kruger, R. G., Lowe, D., Mader, M. M., Marsden, B., Mueller-Fahrnow, A., Müller, S., O'Hagan, R. C., Overington, J. P., Owen, D. R., Rosenberg, S. H., Roth, B., Ross, R., Schapira, M., Schreiber, S. L., Shoichet, B., Sundström, M., Superti-Furga, G., Taunton, J., Toledo-Sherman, L., Walpole, C., Walters, M. A., Willson, T. M., Workman, P., Young, R. N., and Zuercher, W. (2015) The Promise and Peril of Chemical Probes. *Nat. Chem. Biol. 11* (8), 536−541.

(37) Neill, A. L., and Hunt, N. H. (1992) Pathology of Fatal and Resolving *Plasmodium Berghei* Cerebral Malaria in Mice. *Parasitology 105* (Pt 2), 165−175.

K